An Inventory of Global Rocket Launch Emissions and Projected Near-Future Impacts on Stratospheric Ozone

Tyler F. M. Brown[1], Michele T. Bannister[1], Laura E. Revell[1], Timofei Sukhodolov[2,3], Eugene Rozanov[2,4]

[1]Te Kura Matū School of Physical and Chemical Sciences, University of Canterbury, Christchurch, New Zealand
[2]Physikalisch-Meteorologisches Observatorium Davos and World Radiation Center, Davos, Switzerland
[3]Institute of Meteorology and Climatology, University of Natural Resources and Life Sciences, Vienna, Austria
[4]Institute for Atmospheric and Climate Science, ETH Zurich, Zurich, Switzerland

Key Points:

- We compiled an emissions inventory of rocket launches in 2019 and scaled it to explore future impact
- With 2,040 launches per year (120 each from 17 active spaceports), global annual-mean ozone loss is 0.5%
- Arctic springtime ozone loss equates to half of that observed from CFCs in the late 20$^{\text{th}}$ century

Corresponding author: Michele T. Bannister and Laura E. Revell, michele.bannister@canterbury.ac.nz, laura.revell@canterbury.ac.nz

Abstract

The rate of rocket launches is accelerating, driven by the rapid global development of the space industry. Rocket launches emit chemically and radiatively active species into the stratosphere, where they impact ozone. We create a per-vehicle inventory of geographically-resolved stratospheric emissions for 2019, accounting for flight profiles and all major fuel types in active use. The inventory is used to simulate an intensive near-future scenario (120 launches/year at 17 current spaceports) with a chemistry-climate model. These gas-phase rocket emissions produce an overall 0.5% decrease in global annual-mean total column ozone. Compared to a reference scenario, Antarctic springtime ozone decreases by up to 9%. Arctic springtime ozone decreases by up to 5%; equivalent to half of the depletion observed over this region due to chlorofluorocarbons in the late 20$^{\text{th}}$ century. Our findings reiterate the need for assessment and international cooperation regarding the impact of space industrialisation on Earth's systems.

Plain Language Summary

Many governments and companies have expressed bold ambitions to grow their presence in space. However, rocket launches throw out a stream of air pollutants from their burnt fuel as they rise up through the stratosphere, which is where the protective ozone layer resides. Currently, launch operators do not have to measure the impacts of their activities on the ozone layer. We gather together all the publicly available information we can find on rocket launches in 2019 from 17 active spaceports worldwide, and make some careful assumptions to convert each rocket's fuel to its burnt fuel products left in the atmosphere. To explore potential future impacts, we ran a climate model simulation in which each of the 17 spaceports has 120 rocket launches per year. Global average ozone decreases by 0.5%, with larger losses observed in polar regions. Today, the ozone layer is beginning to recover from the chlorofluorocarbons pumped into the atmosphere in the late 20$^{\text{th}}$ century. Our results suggest that sustained and frequent rocket launches in the 21$^{\text{st}}$ century will delay ozone recovery. Careful rocket fuel choices, along with ongoing assessment of stratospheric impacts, could counter this problem.

1 Introduction

Rocket launches lofting payloads to orbit are unique anthropogenic injection points of emissions, emplacing gas and particulates while traveling up through the region of highest ozone concentration (15–35 km) at stratospheric altitudes and beyond. The high reactivity of ozone makes it fragile to reactive species. Ozone absorbs harmful solar UV-B radiation, and is thus essential for the biosphere. Unlike in the troposphere, where mixing, precipitation, and/or chemical oxidation quickly removes emission products, long-lived gases and particulate emissions in the stratosphere, such as from stratovolcanoes or anthropogenic chlorofluorocarbons, can be very destructive (Randel et al., 1995; Molina & Rowland, 1974). They also have widespread effects as the stratosphere is longitudinally well-mixed.

While natural events are singular and transient, rocket launches, though individually smaller, are made far more frequently. The last decade has witnessed 4.8% year-over-year growth in the rate of rocket launches, as commercial entities take a greater role in the expanding global space industry; as of 2022, 12 launch providers are active (McDowell, 2022). Understanding the future impacts of the rocket industry in terms of fuel choices, emissions profiles, and launch cadence is increasingly important as the industry diversifies and grows. Depending on the launch vehicle and fuel type, present rocket launch exhaust can include black carbon, alumina, nitrogen oxides (NO_x = NO + NO_2), reactive chlorine (Cl_x = Cl + ClO), carbon dioxide, and water vapor (Dallas et al., 2020). These species are all either radiatively active or contribute to ozone destruction via chem-

ical reactions (Portmann et al., 2012; Morgenstern et al., 2018; Revell et al., 2012; Tian et al., 2009; Crutzen, 1970; Molina & Rowland, 1974; Solomon, 1999; Yu et al., 2019; Danilin et al., 2001; Carpenter et al., 2018).

Many studies of rocket emissions to date have focused on various impacts of single-fuel emissions or single-species effect, and often from limited injection sites (Prather et al., 1990; Karol et al., 1992; Jackman et al., 1996; Jackman et al., 1998; Ross et al., 2000; Danilin et al., 2001; Danilin et al., 2001; Popp et al., 2002; Ross et al., 2004; M. Ross et al., 2010; Voigt et al., 2013; Larson et al., 2017; Maloney et al., 2021). To capture the effect of the current distribution of spaceports and fuel types on stratospheric ozone, we developed an inventory of emissions products from vehicles in use at currently active spaceports (Section 2.1). We use the inventory to develop a scenario for hypothetical frequent launches at 17 currently active launch sites worldwide, and use this to simulate the gas-phase chemical effects on global stratospheric ozone.

2 Methods

2.1 Development of Baseline Emissions Inventory

We compile a comprehensive inventory of current up-to-date launch vehicles and their stratospheric emissions contributions by mass (Table S2). In total, the catalogue includes 65 vehicles from 11 launcher families, including alternate configurations and contemporary counterparts. We distinguish configurations which have multiple launch locations, e.g. Soyuz at Baikonur versus Kourou, but group those which do not alter the stratospheric emissions burden, e.g. payload fairing size. Launch emissions are calculated on a per-rocket basis, using 2019 as the reference year (McDowell, 2022). As we focus on stratospheric effects, we only consider emission mass injected within 15–50 km altitude.

For each vehicle, we convert the fuel mass of the rocket stages burning within 15–50 km altitude to their experimentally-measured exhaust byproducts as per M. N. Ross and Sheaffer (2014), Desain and Brady (2014), and Larson et al. (2017). For most vehicles, this often means only the first stage and optional booster stages create relevant emissions. The full list of references for the fuel type, propellant mass, and flight profiles for all relevant launch stages is provided (see Section 5). We infer unavailable data from vehicles with similar configuration, similar family, or similar sizing; where necessary, this is specified in Table S3. Alumina conversions are represented as total mass, not only the sub-micron fraction as determined by M. N. Ross and Sheaffer (2014). Differences in solid rocket motor (SRM) mixtures are handled in the same way as Desain and Brady (2014). Stratospheric NO_x conversion rates are from Larson et al. (2017).

The four principal propellant types in use in our catalogue are kerosene-based, cryogenic (LH_2), hypergolic, and solid fuel. We assume that upon launching, the rocket burns its propellant mixture continuously until the entirety of its fuel mass is spent, and that the entirety of this burned fuel is converted to the corresponding emission products in Table 2.1. Due to the combustion reaction in practice burning fuel-rich rather than in stoichiometric ratio, our assumption that all fuel is converted to exhaust products will slightly overestimate the true emissions burden. We use a linear burn profile, ignoring any engine throttling or complexity in plume modeling (Murray et al., 2013; Sheaffer, 2021).

As a rocket ascends to space, it follows a non-linear trajectory towards the desired orbital inclination, dependent on the payload's orbital destination and the location of launch. The choice of flight profile will vary the time spent within the 15-50 km altitude regime, and thus the stratospheric contribution. We selected median flight profiles for each vehicle from among the suite of trajectory options operators offered, cross-referenced with diverse sources on post-launch altitude reports (note the industry convention is to

Fuel Type	**Components**	**Emission Products**	**Prevalence (2019 total propellant mass)**
Kerosene	RP-1 (Kerosene) / LOx	CO_2, H_2O, NO_x, Black Carbon	51%
Cryogenic	LH_2 / LOx	H_2O, H_2, NO_x	7%
Solid	Al / NH_4ClO_4 & HTPB	HCl, H_2O, CO_2, NO_x, Al_2O_3, Black Carbon	12%
Hypergolic	N_2H_4 / UDMH & N_2O_4	H_2O, N_2, CO_2, NO_x, Black Carbon	30%

Table 1. Propellant types and emission products. Relative prevalence shown as percentage of total rocket propellant mass in 2019. SRM-emitted HCl is rapidly converted into Cl_2, which forms reactive chlorine (Cl_x = Cl + ClO).

report launches in burn timing instead of altitude). No suborbital vehicles are included in our inventory, due to their poorly quantified flight profiles. We also omit fuel discrepancies from the boost-back of reusable rockets. This only occurs for Falcon vehicles; they typically reserve <6% of total propellant mass for their stabilization burn (60–30 km) and landing burn (<5 km) (Y. Kim et al., 2021).

While reentry ablation of depleted stages can contribute to NO_x creation, concentrated around altitudes 50 km and above (S.-H. Park et al., 2021), the amount generated is highly dependent on component surface area, geometry, velocity, and mass (S. Kim et al., 2019). Early Space Shuttle estimates of ablative NO_x exist (C. Park & Rakich, 1980), but little data is available for newer vehicles. Due to these factors, we omit ablative NO_x contributions; our outcomes thus have lower NO_x effects relative to those seen in other studies (Ryan et al., 2022; Larson et al., 2017).

The final inventory (Table S2) quantifies the stratospheric contributions by mass of carbon dioxide, water vapor, alumina, black carbon, NO_x, and reactive chlorine, with fine altitude differentiation at per-km resolution. Lastly, the inventory preserves the geolocation of emissions globally, allowing transport of emission species to be assessed. Figure 1 demonstrates how each vehicle contributes a unique combination of exhaust byproducts relative to its emission per launch, balanced with its launch frequency in 2019.

2.2 Atmospheric Modeling

2.2.1 The SOCOLv4 model

We investigated the impacts of rocket emissions on stratospheric ozone with the SOCOLv4 (Solar-Climate Ozone Links version 4) atmosphere-ocean-aerosol-chemistry-

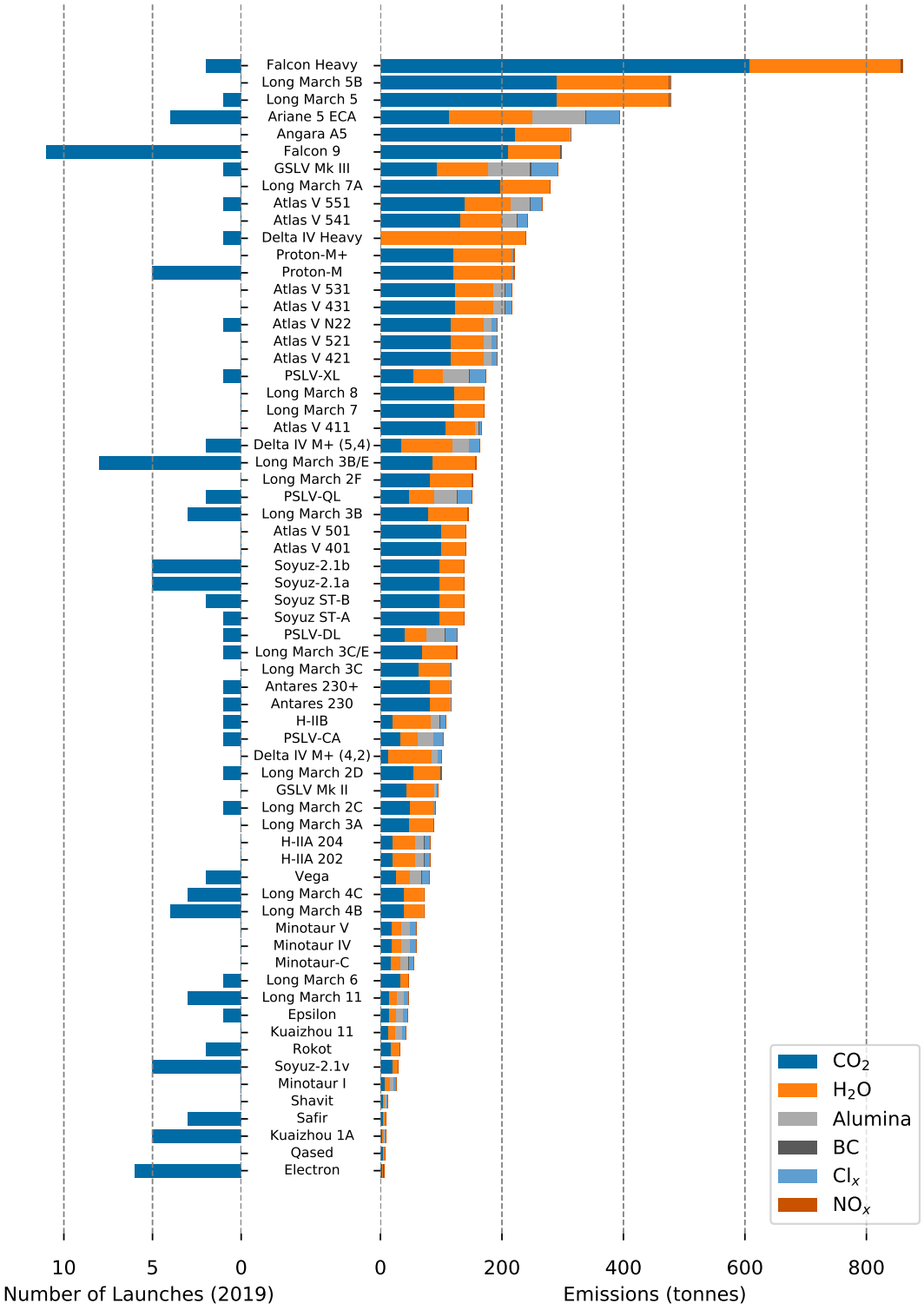

Figure 1. Total emission of each launch vehicle in tonnes. Coloration represents individual emission products (right), with 2019 launch frequency (left). Largest total emission (top) to smallest (bottom) is only a function of vehicle propellant mass, and does not map to ozone impact.

climate model (Sukhodolov et al., 2021). SOCOLv4 is based on the Max Planck Institute Earth System Model version 1.2 (MPI-ESM1.2) (Mauritsen et al., 2019), the sulfate aerosol microphysical model AER (Weisenstein et al., 1997), and includes 99 chemical species from the MEZON chemistry model (Egorova et al., 2003). SOCOLv4 has T63 horizontal resolution, corresponding to approximate grid spacing of $1.9° \times 1.9°$. The atmosphere contains 47 levels from the surface to 0.01 hPa (approximately 80 km) using a hybrid sigma-pressure coordinate system. Overall, SOCOLv4 simulates stratospheric ozone accurately compared with observations (Sukhodolov et al., 2021).

We ran two 30 year time-slice simulations (i.e. with constantly repeating boundary conditions) for the year 2030: a reference simulation, and a simulation with rocket emissions. The 2030 boundary conditions are based on the REFD2 scenario designed for phase 2 of the Chemistry-Climate Model Initiative (Plummer et al., 2021). REFD2 uses greenhouse gas concentrations following the 6^{th} Coupled Model Intercomparison Project (CMIP6) SSP2-4.5 "reference future" scenario (O'Neill et al., 2016), with concentrations of ozone-depleting substances following WMO 2018 (Carpenter et al., 2018). For the rocket emissions simulation, a simulation was first performed using only 2019 gas-phase emissions (Section 2.1). This did not yield any discernible effect on stratospheric ozone. We therefore developed a hypothetical scenario to assess potential impacts of space industry growth.

Input emission mass burdens were gridded as a function of time (monthly mean), pressure, latitude and longitude. The rate of emission per kilometer was calculated from the emission inventory and interpolated to the SOCOLv4 pressure grid. Emissions profiles are provided to the model between 0–50 km for all vehicles. Since SOCOLv4 extends to 80 km above Earth's surface, an exponential decay was added between 50–80 km to approximate post-stratospheric stages. While gas and particulate emissions above the stratopause contribute to stratospheric chemistry (Sinnhuber et al., 2018), they are estimated as minor contributions due to considerably lesser emissions burden from follow-up rocket stages. Emissions files were generated for water vapor, CO_2, NO_x, Cl_x, submicron alumina and black carbon. Because SOCOLv4 does not currently support the inclusion of alumina and black carbon, we focus on the gas-phase emission products only.

2.2.2 Scenario Development

The future stratospheric inputs of the space industry will be dependent, to first order, on growth patterns of vehicle launch cadence versus vehicle propellant mass. This growth is currently economically driven by payload sizing, rocket design, and cost-per-kg to orbit. We developed a near-future launch scenario using the following guidelines:

1. The launch vehicles should represent currently used orbital launch systems. We estimate emission products based solely on currently used vehicles as of 2019 to quantify uncertainty in our projections. Advances in orbital launch systems and new engine designs are a given, whether economically or environmentally driven. However, an approach centered on speculation of the multi-national developmental trajectory of launch platforms, the efficiency and viability of future fuel mixtures, and the mass of vehicles also introduces broad uncertainties. Our approach offers quantification and support from both in-situ measurements and literature.
2. The spaceports should represent current launch sites, which encompass geographically suitable sites with substantive infrastructure investment. Spaceports in Table S1 were chosen from those in operation as of 2019 and which saw at least one launch during that year. By having 17 realistic injection points of emissions, the simulation is able to explore potential geographical effects of launch emissions. Assuredly, new spaceports will develop, with many already planned or beginning operation (Roberts, 2019). That said, future space traffic from each of these sites is similarly difficult to estimate.

3. The vehicles operating at each spaceport should be composed of vehicles currently launched at those spaceports, to approximate legacy strength in industry fuel type usage and fuel balance geographically.
4. The cadence of near-future launch activities should derive from existing regulatory frameworks, to benchmark the outcomes of current legislative thought. Many spaceports do not have a regulated limit on the number of launches: most sites cannot presently accommodate high launch frequency due to logistical or production constraints. However, commercial focus on rapid-cadence launching, reusability, and supply chain improvements indicate this may not always be the case. For instance, New Zealand's Māhia launch site's resource consent permits up to 120 launches/year; operator turnaround capability means these can be within 72 hours (Gugliotta, 2018). We adopt this rate in our scenario. This limit provides a useful benchmark for discussions of sustainability in the international community.
5. A constant rate of launches year-over-year was chosen versus an annual percentage increase in launch activities. The objective of this approach was to quantify effects of the potential emissions burden due to launches that may arise in a variety of ways.

Following the Māhia frequency at each of the 17 currently active launch sites (Fig. 2) totals 2,040 launches annually. This is approximately 20 times current global rates, at 97, 104, 135 launches in 2019, 2020, and 2021 respectively (McDowell, 2022). The global annual burden of each emissions product following this scenario is 138.8 Gg of CO_2, 99.5 Gg of water vapor, 1.1 Gg of black carbon, 0.8 Gg of NO_x, 9.9 Gg of reactive chlorine and 16.1 Gg of alumina.

3 Results and Discussion

As a consequence of sustained frequent rocket launches, global annual-mean total column ozone decreases by 0.53% (1.55 DU). Larger changes in annual-mean total ozone of up to -2.8% are seen at polar latitudes (Fig. 2a). Polar ozone depletion typically maximizes in spring, following conversion of reservoir chlorine to reactive chlorine on the surfaces of polar stratospheric clouds, and is shown in Fig. 2b,c. Springtime total ozone decreases by up to 4.8% and 9% over the Arctic and Antarctic, respectively. The Antarctic stratosphere has experienced significant ozone losses since CFCs entered into widespread use in the 1970s. Our results demonstrate that sustained frequent rocket launches in the near-future would delay recovery of the Antarctic ozone hole, with an 8 DU reduction in October ozone, even though the majority of the launch sites are in the Northern Hemisphere. Over the Arctic we observe an average 13 DU total column ozone loss in March, which is approximately half of the historical ozone depletion seen in March from the mid-1970s to late 1990s (Dhomse et al., 2018). The Arctic rarely experiences ozone holes on the scale seen in the Antarctic, with notable exceptions (Manney et al., 2011, 2020). Additional stratospheric chlorine from launches could deepen these sporadic, dynamically-induced ozone holes in the Arctic. Simulated Arctic ozone losses in March (13 DU) are larger than those over the Antarctic in September (8 DU), likely due to the widespread location of spaceports in the Northern Hemisphere.

Because the largest changes in ozone are seen at polar latitudes during springtime, we examine stratospheric ozone changes as a function of pressure (Fig. 3c,d), as well as the concentrations of reactive chlorine. In the Arctic and Antarctic springtime, the largest percent-wise changes in ozone are in the upper (5 hPa) and lower (100 hPa) stratosphere. These are likely due to chlorine-induced ozone destruction (Fig. 3e,f), as we see significantly larger chlorine concentrations throughout the stratosphere in the rocket launch scenario. NO_x and hydrogen oxides (produced from H_2O) can also destroy stratospheric ozone; however, we do not see significant changes in the concentrations of these species (not shown).

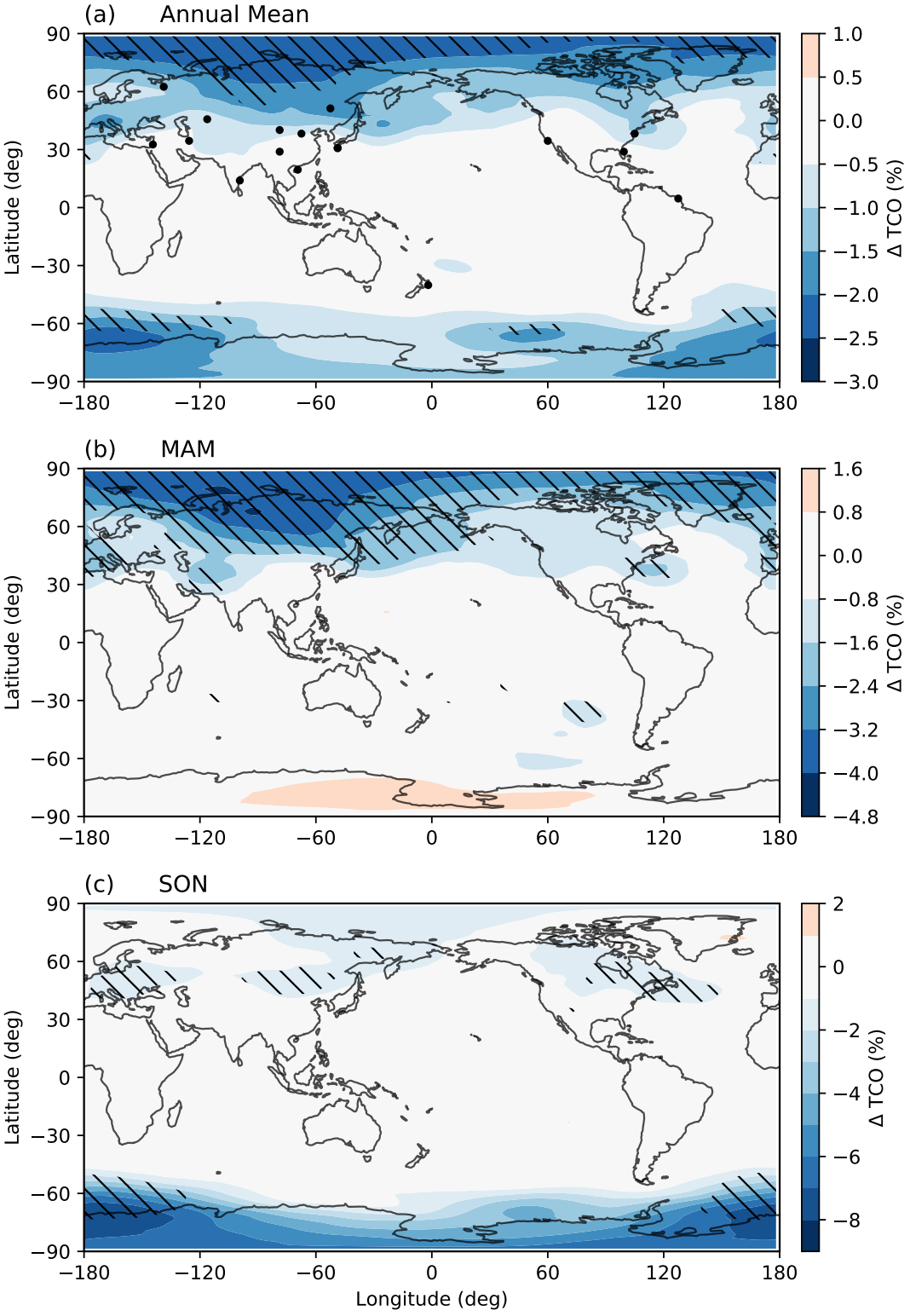

Figure 2. (a) Change in annual-mean total column ozone in the rocket emissions simulation relative to the reference simulation. Black circles indicate launch sites. Two sites, Tanegashima and Uchinoura in Japan, are assigned identical model coordinates because of their real-world proximity. Hatched areas indicate statistical significance (Welch's t-test; 95% level of confidence). (b), (c) as for (a) but for March-May (MAM) and September-November (SON), respectively.

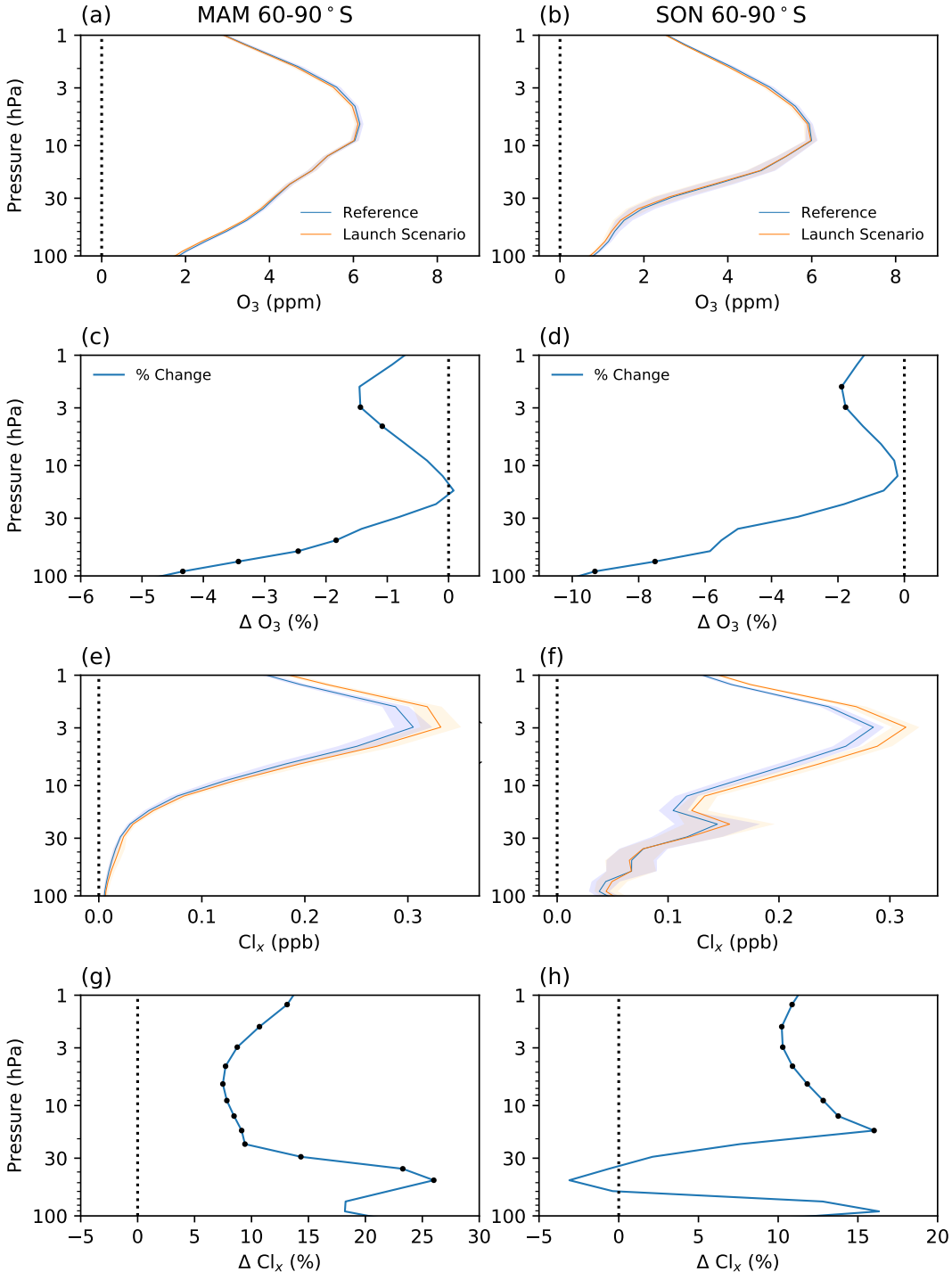

Figure 3. (a) Absolute ozone concentration March-May (MAM) in the Arctic (60-90°N area-weighted average) as a function of pressure. (b) Absolute ozone concentration in September-November (SON) in the Antarctic (60-90°S area-weighted average) as a function of pressure. Black circles indicate a statistically significant change (Welch's t-test; 95% confidence), shaded areas a 95% confidence interval. (c), (d) as for (a), (b) but showing percentage ozone change between launch and reference scenarios. (e) - (h) as for (a–d) but showing Cl_x.

Ross et al. (2004) found that for a launch scenario of 10 Proton vehicles per year, the steady-state ozone loss predicted is small, at 1.2×10^{-4}% per year, associated with NO_x emissions. A 20% decrease in column ozone in the immediate rocket plume was identified, which recovered due to atmospheric mixing. However, NO_x abundances in rocket exhaust are significantly smaller than those produced upon spacecraft and space debris atmospheric reentry (Popp et al., 2002). For launch scenarios considering reentry nitrogen oxide production, a 0.5% loss of global average column ozone was seen, with polar losses exceeding 2% (Larson et al., 2017). Our simulation contained only 0.1% of NO_x mass compared to Larson et al. (2017), which explains our lack of NO_x effects in the simulation.

Hydrogen oxides produced from water vapor oxidation can contribute to ozone loss (Tian et al., 2009), however water vapor can also lead to increases in ozone as it cools the stratosphere. Stratospheric cooling changes the rate of temperature-dependent ozone production and destruction reactions, such that ozone abundances increase. CO_2 has a similar influence on ozone (Portmann et al., 2012; Dhomse et al., 2018). The water vapor addition in our simulation was much less (under 5%) of the global 2 ppmv used by Tian et al. (2009), and did not display notable effects. As well as influencing ozone concentrations, CO_2 and water vapor contribute to climate change: M. N. Ross and Sheaffer (2014) analytically estimated a 16 mW m^{-2} radiative forcing from rocket emissions, with 2% contribution from water vapor, while the CO_2 contribution was negligible. Black carbon and alumina exerted a larger radiative forcing, at 70% and 28%, respectively.

The contribution of chlorine to ozone loss from CFCs is well established: reactive chlorine destroys ozone through gas-phase catalytic cycles (Molina & Rowland, 1974). This is most pronounced in spring in polar regions, when heterogeneous reactions on polar stratospheric clouds during winter lead to a build-up of Cl_2 that is subsequently photolyzed, initiating widespread ozone losses (Farman et al., 1985; Solomon, 1999). The destructive power of rocket-based chlorine has been verified by in-situ measurement of vehicle plumes (Ross et al., 2000). Other simulations focused on global impacts: a 0.4% (12 pptv) increase in background chlorine concentration yielded a 0.14% ozone decrease in the upper stratosphere at northern mid to high latitudes near injection sites (Jackman et al., 1996). A 0.05% polar column ozone decrease was also observed. This is consistent with our results, in which we see polar ozone losses, associated with chlorine increases (26-29 ppt; Fig. 3). The Jackman et al. (1996) scenario encompassed relatively few launches (12 large vehicles per year), suggesting that chlorine-based effects could create even more devastating stratospheric ozone losses with increased launch frequencies.

Because SOCOLv4 is not currently configured to handle black carbon or alumina, these were not included in our simulations. Previous studies indicate that their impacts on stratospheric ozone are substantial, and would likely exacerbate the ozone losses observed in our simulation. Black carbon emitted by both liquid and solid rocket fuels alters atmospheric behavior and contributes to ozone destruction, mainly due to its longevity and warming effects. In a recent study, a singular black carbon injection into the stratosphere (30°N) showed persistent levels of black carbon after 4-6 years of rocket launch activity, with year-round ozone loss of 5-15 DU in the Northern Hemisphere and a potentially more severe Antarctic ozone hole (Maloney et al., 2021). Simulations with an annual stratospheric black carbon emission of 600 metric tons show a 1% depletion in tropical stratospheric ozone and 6% in polar stratospheric ozone (M. Ross et al., 2010). This is approximately half the stratospheric black carbon burden for our rocket emissions scenario (1,100 tons), and yields an ozone response on a similar order of magnitude to our gas-phase only simulation. We speculate that the addition of black carbon to our simulations may therefore increase ozone losses by a factor of 3, however noting that stratospheric chemistry is highly non-linear and the impacts of gas-phase products are expected to be altered by black carbon heating of the stratosphere.

Alumina particles from SRMs indirectly contribute to ozone depletion, by acting as a surface medium for chlorine activation. Alumina particles provide sites to catalyze the $ClONO_2 + HCl \rightarrow HNO_3 + Cl_2$ reaction. Both Cl_x and alumina particulates are emitted together in SRM exhaust wakes, compounding the ozone losses that occur (Danilin et al., 2001). Expanding globally, this effect was demonstrated using 2-D photochemistry transport models through infrequent launch burden scenarios of SRM-equipped launch vehicles. Annual average global ozone decreased by 0.025%, due to both alumina particulates and chlorine in tandem (Jackman et al., 1998). Of particular importance in assessing alumina-driven destruction of ozone is particle size: only the sub-micron fraction of alumina in the stratosphere contribute to regional chemical processes (M. N. Ross & Sheaffer, 2014; Schmid et al., 2003). While the total alumina burden is well-understood for SRM emission, particle size distributions are not. Future studies should revisit the sensitivity of stratospheric ozone to sub-micron alumina from SRM, given planned launches. Deorbiting satellite constellations will provide another source of sub-micron alumina, which should also be examined (Boley & Byers, 2021; S.-H. Park et al., 2021).

4 Conclusions

We present a current inventory of stratospheric emission products from global rocket launches. The emissions inventory includes vehicle data and granular flight profiles for every orbital launch system used as of 2019, and encompasses the four major fuel types currently in use (liquid kerosene, cryogenic, hypergolic, and solid). The inventory presents a global snapshot of current launch activity, and provides a data set with which to explore potential future emission scenarios.

The inventory was scaled to represent a hypothetical near-future launch scenario, with 120 launches per year at each of the 17 currently active spaceports (all but one of which are in the Northern Hemisphere). The scenario is aggressive, but realistic: it uses real launch vehicle emissions, active spaceports, and a launch cadence enacted in New Zealand licensing. Chemistry-climate modeling with this scenario yields a 0.5% decrease in global annual-mean total column ozone. More severe losses are seen in polar regions during springtime, mainly due to the presence of SRM-emitted reactive chlorine. Antarctic ozone in October decreases by up to 9%, while Arctic ozone in March decreases by up to 5%. The Arctic ozone losses are half those seen in the last decades of the 20^{th} century due to CFCs. Frequent and sustained future rocket launches may therefore partially offset the gains achieved through the Montreal Protocol for Substances that Deplete the Ozone Layer, and delay ozone recovery. In our simulations we accounted only for gas-phase emission products (CO_2, water vapor, reactive chlorine and NO_x). Future modeling should assess the impacts of fuel-emitted black carbon and alumina (currently in development for SOCOLv4), along with further impact of NO_x generated from spacecraft reentry; the collective atmospheric impact of ablative reentry may soon grow in importance with massive satellite constellation build-outs.

To create a sustainable space economy, the rocket launches that form the core of space industrialization must achieve and maintain high standards of environmental sustainability. The industry would benefit from a more holistic understanding of sustainability, including accounting for the impact of terrestrial operations on Earth's ecosystems, both in launch and in demisability. This work suggests that there is potential to develop standard operator best-practice in collaboration with atmospheric scientists. Publicly available characterisation of the emission products of new vehicles will be key — such as the upcoming SpaceX Starship, which is five times as massive as the median vehicle (by propellant mass) in our inventory, and uses a uncharacterized methane fuel type (SpaceX, 2022). For vehicles in this size class, even an infrequent launch cadence could have substantial effects on the global emissions burden. Determining the ongoing effects of rocket emissions is essential to ensure the future integrity of the stratospheric ozone layer and the protection it provides to the biosphere.

5 Data Availability

Full simulation data output for launch and reference scenarios, emissions inventory tables, and vehicle-specific references for the dataset beyond the Supporting Information are available at https://doi.org/10.5281/zenodo.6499777.

Acknowledgments

TS and ER were supported by the Swiss National Science Foundation (SNSF) (POLE (grant no. 200020-182239)). SOCOLv4 model calculations were supported by the Swiss National Supercomputing Centre (CSCS) under project S-1029 (ID 249). Part of the simulations were performed on the ETH Zürich cluster EULER. TFMB received financial support from the University of Canterbury. MTB appreciates support by the Rutherford Discovery Fellowships from New Zealand Government funding, administered by the Royal Society Te Apārangi. MTB and LER thank Martin Ross and Leonard David for their Scientific American article (November 2020), 'An Underappreciated Danger of the New Space Age: Global Air Pollution', which sparked the curiosity that led to this research.

References

Boley, A. C., & Byers, M. (2021). Satellite mega-constellations create risks in Low Earth Orbit, the atmosphere and on Earth. *Scientific Reports*, *11*(1), 10642. doi: 10.1038/s41598-021-89909-7

Carpenter, L., Daniel, J., Fleming, E., Hanaoka, T., Hu, J., Ravishankara, A., ... Wuebbles, D. (2018). Scenarios and Information for Policymakers, Chapter 6 in Scientific Assessment of Ozone Depletion: 2018.

Crutzen, P. J. (1970). The influence of nitrogen oxides on the atmospheric ozone content. *Quarterly Journal of the Royal Meteorological Society*, *96*(408), 320-325. doi: https://doi.org/10.1002/qj.49709640815

Dallas, J. A., Raval, S., Alvarez Gaitan, J. P., Saydam, S., & Dempster, A. G. (2020). The environmental impact of emissions from space launches: A comprehensive review. *Journal of Cleaner Production*, *255*, 120209. doi: 10.1016/j.jclepro.2020.120209

Danilin, M. Y., Ko, M. K. W., & Weisenstein, D. K. (2001). Global implications of ozone loss in a space shuttle wake. *Journal of Geophysics Research*, *106*(D4), 3591-3601. doi: 10.1029/2000JD900632

Danilin, M. Y., Shia, R. L., Ko, M. K. W., Weisenstein, D. K., Sze, N. D., Lamb, J. J., ... Prather, M. J. (2001). Global stratospheric effects of the alumina emissions by solid-fueled rocket motors. *Journal of Geophysics Research*, *106*(D12), 12,727-12,738. doi: 10.1029/2001JD900022

Desain, J., & Brady, B. (2014). *Potential Atmospheric Impact Generated by Space Launches Worldwide—Update for Emission Estimates from 1985 to 2013* (Tech. Rep.). El Segundo, California: The Aerospace Corporation.

Dhomse, S. S., Kinnison, D., Chipperfield, M. P., Salawitch, R. J., Cionni, I., Hegglin, M. I., ... Zeng, G. (2018). Estimates of ozone return dates from Chemistry-Climate Model Initiative simulations. *Atmospheric Chemistry and Physics*, *18*(11), 8409–8438. doi: 10.5194/acp-18-8409-2018

Egorova, T., Rozanov, E., Zubov, V., & Karol, I. (2003, 05). Model for investigating ozone trends (MEZON). *Izvestiya - Atmospheric and Ocean Physics*, *39*, 277-292.

Farman, J. C., Gardiner, B. G., & Shanklin, J. D. (1985). Large losses of total ozone in Antarctica reveal seasonal ClOx/NOx interaction. *Nature*, *315*(6016), 207–210. Retrieved from `https://doi.org/10.1038/315207a0` doi: 10.1038/315207a0

Gugliotta, G. (2018). *Small Rockets Aim for a Big Market.* Retrieved 2022-03-30, from https://www.smithsonianmag.com/air-space-magazine/milestone-180968351/

Jackman, C. H., Considine, D. B., & Fleming, E. L. (1996). Space shuttle's impact on the stratosphere: An update. *Journal of Geophysics Research*, *101*(D7), 12,523-12,529. doi: 10.1029/96JD00577

Jackman, C. H., Considine, D. B., & Fleming, E. L. (1998). A global modeling study of solid rocket aluminum oxide emission effects on stratospheric ozone. *Geophysical Research Letters*, *25*(6), 907-910. doi: https://doi.org/10.1029/98GL00403

Karol, I. L., Ozolin, Y. E., & Rozanov, E. V. (1992, October). Effect of space rocket launches on ozone. *Annales Geophysicae*, *10*(10), 810-814. Retrieved from https://ui.adsabs.harvard.edu/abs/1992AnGeo..10..810K

Kim, S., Jo, B.-U., Choi, E.-J., Cho, S., & Ahn, J. (2019). Two-phase framework for footprint prediction of space object reentry. *Advances in Space Research*, *64*(4), 824-835. doi: https://doi.org/10.1016/j.asr.2019.05.023

Kim, Y., Lee, H.-J., & Roh, T.-S. (2021). Analysis of Propellant Weight under Re-Entry Conditions for a Reusable Launch Vehicle Using Retropropulsion. *Energies*, *14*(11). doi: 10.3390/en14113210

Larson, E. J. L., Portmann, R. W., Rosenlof, K. H., Fahey, D. W., Daniel, J. S., & Ross, M. N. (2017). Global atmospheric response to emissions from a proposed reusable space launch system. *Earth's Future*(5), 37 – 48. doi: 10.1002/2016EF000399

Maloney, C., Portmann, R. W., Ross, M., & Rosenlof, K. H. (2021, December). The Climate and Ozone Impacts of Black Carbon Emissions from Global Rocket Launches. In *Agu 2021 fall meeting.*

Manney, G. L., Livesey, N. J., Santee, M. L., Froidevaux, L., Lambert, A., Lawrence, Z. D., ... Fuller, R. A. (2020). Record-Low Arctic Stratospheric Ozone in 2020: MLS Observations of Chemical Processes and Comparisons With Previous Extreme Winters. *Geophysical Research Letters*, *47*(16). doi: https://doi.org/10.1029/2020GL089063

Manney, G. L., Santee, M. L., Rex, M., Livesey, N. J., Pitts, M. C., Veefkind, P., ... Zinoviev, N. S. (2011). Unprecedented Arctic ozone loss in 2011. *Nature*, *478*(7370), 469–475. doi: 10.1038/nature10556

Mauritsen, T., Bader, J., Becker, T., Behrens, J., Bittner, M., Brokopf, R., ... Roeckner, E. (2019). Developments in the MPI-M Earth System Model version 1.2 (MPI-ESM1.2) and Its Response to Increasing CO2. *Journal of Advances in Modeling Earth Systems*, *11*(4), 998-1038. doi: https://doi.org/10.1029/2018MS001400

McDowell, J. (2022). *Jonathan's Space Report.* Retrieved 2022-03-28, from https://www.planet4589.org/space/index.html

Molina, M. J., & Rowland, F. S. (1974). Stratospheric sink for chlorofluoromethanes: chlorine atom-catalysed destruction of ozone. *Nature*, *249*(5460), 810–812. Retrieved from https://doi.org/10.1038/249810a0 doi: 10.1038/249810a0

Morgenstern, O., Hegglin, M. I., Rozanov, E., O'Connor, F. M., Abraham, N. L., Akiyoshi, H., ... Zeng, G. (2018). Review of the global models used within phase 1 of the Chemistry–Climate Model Initiative (CCMI). *Geoscientific Model Development*, *10*(2), 639–671. doi: 10.5194/gmd-10-639-2017

Murray, N., Bekki, S., Toumi, R., & Soares, T. (2013). On the uncertainties in assessing the atmospheric effects of launchers. *EUCASS Proceedings Series*, *4*, 671-688. doi: 10.1051/eucass/201304671

O'Neill, B. C., Tebaldi, C., van Vuuren, D. P., Eyring, V., Friedlingstein, P., Hurtt, G., ... Sanderson, B. M. (2016). The Scenario Model Intercomparison Project (ScenarioMIP) for CMIP6. *Geoscientific Model Development*, *9*(9), 3461–3482. doi: 10.5194/gmd-9-3461-2016

Park, C., & Rakich, J. V. (1980). Equivalent-cone calculation of nitric oxide production rate during space shuttle re-entry. *Atmospheric Environment (1967)*, *14*(8), 971-972. doi: https://doi.org/10.1016/0004-6981(80)90011-6

Park, S.-H., Navarro Laboulais, J., Leyland, P., & Mischler, S. (2021). Re-entry survival analysis and ground risk assessment of space debris considering by-products generation. *Acta Astronautica*, *179*, 604-618. doi: https://doi.org/10.1016/j.actaastro.2020.09.034

Plummer, D., Nagashima, T., Tilmes, S., Archibald, A., Chiodo, G., Fadnavis, S., ... Peter, T. (2021). CCMI-2022: A new set of Chemistry-Climate Model Initiative (CCMI) Community Simulations to Update the Assessment of Models and Support Upcoming Ozone Assessment Activities. *SPARC Newsletter*, *58*, 39. Retrieved from `https://www.sparc-climate.org/publications/newsletter/sparc-newsletter-no-57/`

Popp, P. J., Ridley, B. A., Neuman, J. A., Avallone, L. M., Toohey, D. W., Zittel, P. F., ... Danilin, M. Y. (2002). The emission and chemistry of reactive nitrogen species in the plume of an Athena II solid-fuel rocket motor. *Geophysics Research Letters*, *29*(18), 1887. doi: 10.1029/2002GL015197

Portmann, R. W., Daniel, J. S., & Ravishankara, A. R. (2012). Stratospheric ozone depletion due to nitrous oxide: influences of other gases. *Philosophical Transactions: Biological Sciences*, *367*(1593), 1256–1264.

Prather, M. J., Garcia, M. M., Douglass, A. R., Jackman, C. H., Ko, M. K. W., & Sze, N. D. (1990). The space shuttle's impact on the stratosphere. *J. Geophys. Res.*, *95*, 18583–18590. doi: 10.1029/JD095iD11p18583

Randel, W. J., Wu, F., Russell III, J. M., Waters, J. W., & Froidevaux, L. (1995). Ozone and temperature changes in the stratosphere following the eruption of Mount Pinatubo. *Journal of Geophysical Research: Atmospheres*, *100*(D8), 16753-16764. doi: https://doi.org/10.1029/95JD01001

Revell, L. E., Bodeker, G. E., Huck, P. E., Williamson, B. E., & Rozanov, E. (2012). The Sensitivity of Stratospheric Ozone Changes Through the 21st Century to N_2O and CH_4. *Atmospheric Chemistry and Physics*, *12*(23), 11309–11317. doi: 10.5194/acp-12-11309-2012

Roberts, T. G. (2019). *Spaceports of the World* (Tech. Rep.). Washington, D.C.: Center for Strategic & International Studies: CSIS Aerospace Security Project.

Ross, M., Mills, M., & Toohey, D. (2010). Potential climate impact of black carbon emitted by rockets. *Geophysical Research Letters*, *37*(24), 1–6. doi: 10.1029/2010GL044548

Ross, M. N., Danilin, M. Y., Weisenstein, D. K., & Ko, M. K. W. (2004). Ozone depletion caused by NO and H2O emissions from hydrazine-fueled rockets. *Journal of Geophysical Research: Atmospheres*, *109*(D21). doi: https://doi.org/10.1029/2003JD004370

Ross, M. N., & Sheaffer, P. M. (2014). Radiative forcing caused by rocket engine emissions. *Earth's Future*, *2*(4), 177–196. doi: 10.1002/2013ef000160

Ross, M. N., Toohey, D. W., Rawlins, W. T., Richard, E. C., Kelly, K. K., Tuck, A. F., ... Sheldon, W. R. (2000). Observation of stratospheric ozone depletion associated with Delta II rocket emissions. *Geophysics Research Letters*, *27*(15), 2209-2212. doi: 10.1029/1999GL011159

Ryan, R. G., Marais, E. A., Balhatchet, C. J., & Eastham, S. D. (2022). Impact of Rocket Launch and Space Debris Air Pollutant Emissions on Stratospheric Ozone and Global Climate. *ESSOAR pre-print (submitted to Earth's Future)*, 23. doi: 10.1002/essoar.10510460.1

Schmid, O., Reeves, J. M., Wilson, J. C., Wiedinmyer, C., Brock, C. A., Toohey, D. W., ... Ross, M. N. (2003). Size-resolved particle emission indices in the stratospheric plume of an Athena II rocket. *Journal of Geophysical Research (Atmospheres)*, *108*(D8), 4250. doi: 10.1029/2002JD002486

Sheaffer, P. M. (2021). Garbage-In Garbage-Out (GIGO): The Use and Abuse of Combustion Modeling and Recent U.S. Spacelaunch Environmental Impacts. *AGU 2021 Fall Meeting (via ESSOAR)*, 18. doi: 10.1002/essoar.10509138.9

Sinnhuber, M., Berger, U., Funke, B., Nieder, H., Reddmann, T., Stiller, G., ... Wissing, J. M. (2018). NO_y production, ozone loss and changes in net radiative heating due to energetic particle precipitation in 2002–2010. *Atmospheric Chemistry and Physics*, *18*(2), 1115–1147. doi: 10.5194/acp-18-1115-2018

Solomon, S. (1999). Stratospheric ozone depletion: A review of concepts and history. *Reviews of Geophysics*, *37*(3), 275-316. doi: https://doi.org/10.1029/1999RG900008

SpaceX. (2022). *Spacex starship.* Retrieved 2022-03-31, from `https://www.spacex.com/vehicles/starship/`

Sukhodolov, T., Egorova, T., Stenke, A., Ball, W. T., Brodowsky, C., Chiodo, G., ... Rozanov, E. (2021). Atmosphere–ocean–aerosol–chemistry–climate model SOCOLv4.0: description and evaluation. *Geoscientific Model Development*, *14*(9), 5525–5560. doi: 10.5194/gmd-14-5525-2021

Tian, W., Chipperfield, M. P., & Lü, D. (2009). Impact of increasing stratospheric water vapor on ozone depletion and temperature change. *Advances in Atmospheric Sciences*, *26*(3), 423–437. doi: 10.1007/s00376-009-0423-3

Voigt, C., Schumann, U., Graf, K., & Gottschaldt, K.-D. (2013). Impact of rocket exhaust plumes on atmospheric composition and climate — an overview. *Progress in Propulsion Physics*, *4*, 657–670. doi: 10.1051/eucass/201304657

Weisenstein, D. K., Yue, G. K., Ko, M. K. W., Sze, N.-D., Rodriguez, J. M., & Scott, C. J. (1997). A two-dimensional model of sulfur species and aerosols. *Journal of Geophysical Research: Atmospheres*, *102*(D11), 13019-13035. doi: https://doi.org/10.1029/97JD00901

Yu, P., Toon, O., Bardeen, C., Zhu, Y., Rosenlof, K., Portmann, R., ... Robock, A. (2019). Black carbon lofts wildfire smoke high into the stratosphere to form a persistent plume. *Science*, *365*, 587-590. doi: 10.1126/science.aax1748